Advanced Carbon Journal, 2026, Vol. x, Iss. x, 165-190

DOI: 10.62184/acj.jacj1000202524

Review Article

SCIENCE PARK PUBLISHER

Advanced Carbon Journal

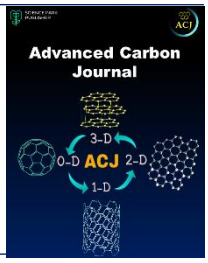

Advances in carbon-based bioinks for bioprinting: Rheology, printability, and applications

Kami Bartholomew[#] and Anil Mahapatro*

Department of Biomedical Engineering, Wichita State University, Wichita, KS-67260

Received: 26, 08, 2025; Accepted: 20, 01, 2026; Published: 13, 03, 2026

Abstract

Bioprinting is a rapidly advancing field within tissue engineering that enables the precise, layer- by-layer deposition of biomaterials, analogous to conventional three-dimensional (3D) printing techniques. A variety of bioprinting modalities and material systems are employed depending on the targeted application. The materials used in this process are referred to as bioinks. Carbon-based bioinks typically consist of one or more hydrogel matrices, which may be synthetic, such as poly(ethylene glycol) diacrylate (PEGDA) and poly(L-lactic acid) (PLLA), or naturally derived, including alginate, collagen, and gelatin. In recent years, carbon-based nanomaterials, such as graphene, graphene oxide (GO), carbon nanotubes (CNTs), carbon dots (CDs), and nanodiamonds (NDs), have emerged as multifunctional additives in hydrogel-based bioinks, offering enhanced mechanical, electrical, and biological properties. These materials must meet certain requirements and have specific properties to be successful bioinks. Bioinks must be biocompatible, so as to not damage cells, and biomimetic to promote cellular proliferation, adhesion, and other cellular activities. Bioinks must also have favorable rheological properties which describe the material's behavior. If a material is too viscous, too thin, or does not have the appropriate viscoelastic properties, it will not be able to be extruded from the bioprinter and might not provide the mechanical strength needed to support cellular activity. Once the bioink has been proven to have favorable biological and material properties, the bioinks can be customized by adding different cell types and growth factors, making them suitable for multiple applications including bioprinting cardiovascular constructs, cartilage and bone constructs, and cancer models. Bioprinting is an interdisciplinary field that involves collaboration among researchers from various disciplines. This manuscript aims to provide a brief introduction to the field while identifying research trends across various aspects of bioprinting.

Keywords: Bioprinting; Carbon nanomaterials; Bioinks; Rheology; Printability; Bioprinted cancer model

1. Introduction

1.1. History of Bioprinting

Additive manufacturing, more commonly called three-dimensional (3D) printing, is a manufacturing technique that places single layers of material on top of one another until the desired shape or part has been produced. Each layer is dispensed onto a platform, frequently called the print bed. Print beds typically move in the z-direction, allowing the layers to be stacked, while the print nozzle typically moves in the x- and y-directions. These shapes and parts are first modeled in a computer-aided design (CAD) software. The CAD part is then processed and turned into G-code that informs the 3D printer the exact location that each layer should

Advanced Carbon Journal, 2026, Vol. x, Iss. x, 165-190
DOI: 10.62184/acj.jacj1000202524

be deposited. 3D printing technology was developed in the 1980s and has been increasing in popularity since then [1]. 3D printing uses materials such as plastics, metals, or ceramics and has made its way into a variety of fields such as engineering, manufacturing, and the medical field [1, 2]. 3D printing enables the rapid creation of prototypes, accurate and precise models, and personalized products while also allowing for parts to be made quickly and repeatably.

After 20 years, additive manufacturing made its way into the field of tissue engineering. 3D printing was adopted as a technique to produce 3D scaffolds with embedded cells; this process is called bioprinting [3]. Similarly, to traditional 3D printing, bioprinting is a technique that places single layers of material on top of one another to produce the desired shape. A big advantage that bioprinting has over other tissue engineering techniques, it allows for the control of cell placement and cell density within a printed construct [4, 5]. Bioprinting utilizes materials that are biocompatible and often biomimetic as a measure to keep the cells alive and allowing them to adhere and proliferate after being bioprinted. These materials, called bioinks, are typically hydrogels, which are materials consisting mostly of water. Hydrogels can be made from a variety of materials, each having different properties, making them suitable for different applications. Before bioprinting, cells are mixed into the bioink. The bioink and cells are then printed together to form a scaffold, which supports the cells as they grow and eventually take over the construct. Some bioprinters allow for two or more different inks to be extruded at the same time [6], enabling ink combinations to be used to create scaffolds with higher degrees of customization.

In recent years, carbon-based nanomaterials, including graphene, graphene oxide (GO), carbon nanotubes (CNTs), carbon dots (CDs), and nanodiamonds (NDs), have gained increasing attention as multifunctional additives in hydrogel-based bioinks [7-12]. These nanomaterials have been shown to significantly enhance the mechanical strength, electrical conductivity, and rheological stability of bioinks, while also promoting improved cellular responses such as adhesion, proliferation, and differentiation. Additionally, their high surface area, tunable surface chemistry, and the ability to interact with polymer networks enable precise modulation of printability and structural fidelity, making carbon-based nanomaterials promising components for advanced bioprinting applications, particularly in electrically active and mechanically demanding tissues.

1.2. Bioprinters

There are different types of bioprinters used in bioprinting, including inkjet, extrusion, laser-assisted, and stereolithography (SLA) systems. Each type of printer has pros and cons when it comes to bioprinting applications. Different types of bioprinters can handle a different range of bioink viscosities, cell densities and printing speeds [13]. An overview of printer properties can be seen in table 1.

Inkjet bioprinters work in a way that is similar to traditional desktop inkjet printers. Inkjet bioprinters dispense successive drops of bioink onto the print bed, using heat or piezoelectric actuation to expel the drops, as seen in Figure 1. The printer dispenses the droplets in a pattern specified by a CAD model. These printers lack precision, as the printer struggles to dispense each bioink drop in an exact location. While inkjet printers are relatively safe for cells and are available at a low cost, they require bioinks with low viscosities, limiting the materials that can be used [1, 3, 14]. Low viscosity materials are required to prevent the nozzle from getting clogged.

Table 1. A comparison of bioprinters with respect to their cost, cell viability, print resolution, and print speed [13]. The values represent general ranges and are not device specific.

Property	Inkjet	Extrusion	Laser	SLA
Cost	Low	Medium	High	Low
Cell Viability	>85%	40%–80%	>95%	>85%
Resolution	High	Medium	High	High
Print Speed	Fast	Slow	Medium	Fast

Advanced Carbon Journal, 2026, Vol. x, Iss. x, 165-190
DOI: 10.62184/acj.jacj1000202524

Review Article

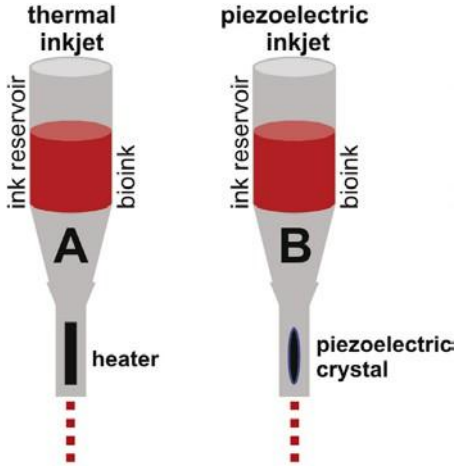

Figure 1. Inkjet bioprinters dispense the bioink in small droplets, much like a standard inkjet printer.

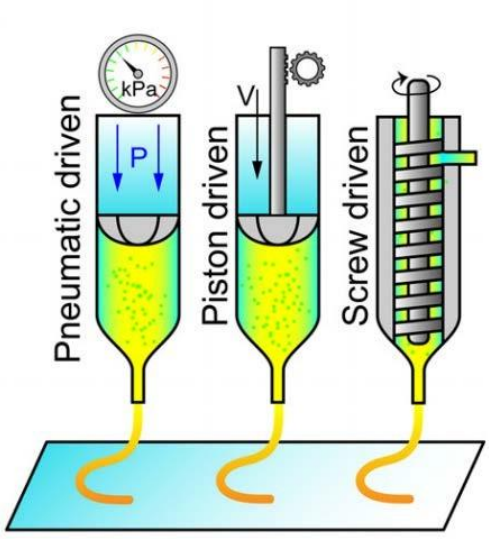

Figure 2. The three types of extrusion all dispense the bioink in a continuous stream, but they use different mechanisms to push the bioink through the nozzle. Adapted from Ref [15], copyright AIP Publishing.

Extrusion bioprinters push the bioink out of the nozzle in a continuous stream directly onto the print bed following the CAD specified pattern. Unlike inkjet bioprinters, extrusion bioprinters can handle viscous bioinks [2].

Extrusion bioprinters are the most commonly used type of bioprinter [2]. There are different types of extrusion bioprinters, characterized based on the way the extrusion force is produced. One type of extrusion bioprinter uses a pneumatic force, also known as air pressure, to push the bioink through the nozzle. Another type of extrusion bioprinter uses a piston to produce a mechanical force on the bioink to extrude it through the nozzle [3, 15]. The third type of extrusion bioprinter utilizes a threaded screw mechanism to feed the bioink through the nozzle and onto the platform. Each type of extrusion bioprinter can be seen in Figure 2. Extrusion bioprinters are more precise than inkjet bioprinters but exert a higher force onto the bioink as it is pushed through the nozzle, which in turn subjects the cells to high forces [16]. These forces can decrease cellular viability, which decreases the viable cell density in the printed construct. On the other hand, extrusion bioprinters allow for the use of multiple printing techniques. Direct bioprinting is the most used technique and is the layer-by-layer deposition of the bioink directly onto the print bed. Coaxial printing is the use of a nozzle with a concentric tube in the center. As the bioink is extruded out, the center tube prevents the center of the layer from being filled,

like a donut. This allows for the printing of tubular structures, which can be used to mimic vasculature [3, 17, 18]. Sacrificial bioprinting, also called indirect bioprinting utilizes two different bioinks, a scaffold material and a sacrificial material, to create hollow or porous structures. In sacrificial bioprinting, the scaffold and the sacrificial ink are used to print one construct. The scaffold is cured and then the construct is placed in a solution that will dissolve the sacrificial ink. Once the sacrificial ink is dissolved, the construct is removed from the solution and often rinsed with saline or phosphate buffered saline (PBS) to remove any remaining sacrificial ink [3, 19-21].

Another type of bioprinter is the laser-assisted bioprinter. This type of bioprinter utilizes a laser pulse to propel bioink droplets off a ribbon and onto the print bed, which can be seen in Figure 3 [15]. Laser-assisted bioprinting is very precise and is nozzle free, so it is able to print with viscous bioinks. Laser-assisted bioprinting is very expensive compared to other bioprinting methods and can result in low cell viability due to the cells' exposure to the high energy laser pulses.

The last type of bioprinter is stereolithography (SLA). SLA uses lasers or ultraviolet (UV) light to polymerize, or harden, a liquid polymer. As each layer is polymerized, the platform is lowered to allow more liquid to flood the platform and be polymerized in a CAD specified pattern. This can be seen in Figure 4. While this method is very precise, SLA exposes cells to high levels of radiation, which can affect cell viability. SLA bioprinting also has a limited number of compatible bioinks, due to the need for photosensitive materials [22].

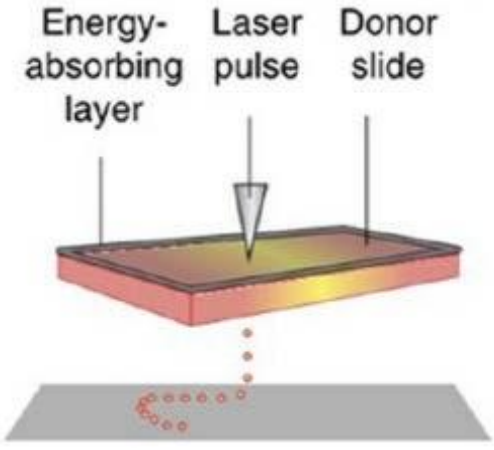

Figure 3. Laser assisted bioprinters use laser pulses instead of a nozzle to dispense bioink onto the print bed [16]. Open access article distributed under the Creative Commons Attribution License.

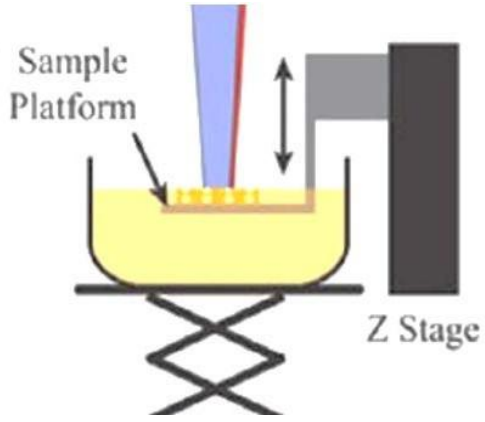

Figure 4. Stereolithography bioprinters cure each layer as it is placed on top of the preceding layer. Adapted from Ref [3], copyright ACS Publications.

DOI: 10.62184/acj.jacj1000202524

2. Bioinks

Bioinks are the materials used for bioprinting and are typically hydrogel-based systems [23]. Hydrogels are materials that have an ability to absorb a water, giving them a high water content [24]. Bioinks must undergo physical or covalent crosslinking to form three dimensional constructs and be able to maintain their shape [3, 25, 26]. A variety of materials can be made into hydrogels, and it is often a combination of materials that allows for the hydrogel to be printable while also promoting cellular activity [1]. There are two types of materials that can be used to make hydrogels, synthetic and natural materials [19, 27]. Synthetic materials are man-made while natural materials are derived from plants or animals. Each type of material has properties that are advantageous for bioprinting and some that are disadvantageous.

2.1. Bioink properties

Many bioinks are designed to recreate the in vivo environment by mimicking the structural, chemical, and biological properties of the extracellular matrix [16, 28, 29]. Bioinks also tend to be viscoelastic, meaning they exhibit both solid and liquid behaviors [23]. While many materials with excellent mechanical properties and high printability exist for traditional 3D printing, there is still room to improve the properties of bioinks [2]. 3D bioprinted constructs must have some degree of mechanical strength to prevent the construct from collapsing on itself. Printed constructs must also be mechanically stable enough to support cell adhesion and growth [23]. The degree of mechanical stiffness and stability required varies depending on the application [2]. Rheological properties describe the viscoelasticity and flow dynamics of hydrogels [26]. There are multiple rheological properties that indicate if a bioink can be printed [23]. Hydrogels suitable for bioprinting must exhibit shear-thinning behavior, meaning that as the force or shear stress on the materials increases, the viscosity decreases [25, 26]. Shear-thinning behavior allows the bioink to be easily extruded through the printer nozzle, where forces are high, while allowing the construct to keep its shape after being printed when the forces are low. Yield stress is another important rheological property in bioprinting. Yield stress is the point at which a hydrogel no longer behaves elastically, and it starts to flow [26]. High yield stress has been linked to high quality printed constructs. This is due to the material's ability to maintain its elasticity as it experiences the weight of successively printed layers. Bioinks with a low yield stress are more prone to losing their shape once under the weight of the rest of the printed construct [30]. Viscosity recovery is another rheological property important to bioprinting. As a bioink is printed it experiences very little shear stress, then a high shear stress while being printed, and then another period of low shear stress after being printed. If the bioink is shear-thinning, the viscosity will decrease during printing. After printing, the viscosity should return to its pre-printed value; if this does not occur, then the bioink will not be able to hold its shape, resulting in poor printability [26]. Biocompatibility is a term used to describe materials that do not cause adverse effects on cells [2]. All bioinks must be biocompatible, but bioinks should have positive effects on cells, such as promoting adhesion and proliferation while mimicking native extracellular matrix [1, 27, 31, 32]. Creating an environment that closely resembles a cell's native environment is known as biomimicry. Biomimicry enables cells to behave as they would in in vivo environments, allowing them to thrive [2]. A summary of these properties can be seen in Table 2.

2.2. Carbon-based bioinks

Carbon-based nanomaterials, such as graphene, graphene oxide (GO), carbon nanotubes (CNTs), carbon dots (CDs), and nanodiamonds (NDs), have emerged as multifunctional additives for hydrogel bioinks. Even at low concentrations, typically below 0.5 wt%, these fillers markedly enhance rheological behavior, print fidelity, mechanical robustness, and in some cases electrical conductivity—properties that are crucial for electroactive tissue constructs and cell viability [8, 10, 12]. GO in particular improves viscosity and resolution in alginate/gelatin, gellan gum, and collagen systems, supporting high cell viability and microarchitecture fidelity [8, 10]. CNTs act as conductive reinforcers, with hyaluronic-acid/MWCNT bioinks demonstrating superior mechanical strength and cell compatibility for cartilage constructs when dispersion and endotoxin levels are properly controlled [9]. Carbon dots extend functionality further by serving as visible-light photoinitiators for protein-based hydrogels such as silk fibroin, enabling gentle crosslinking and intrinsic fluorescence for bioimaging [11]. Nanodiamonds, being sp^3-

bonded and chemically inert, improve the toughness and cell adhesion of gelatin hydrogels, showing promise for long-term stability in extrusion-printed scaffolds [7]. Thus, carbon nanomaterials offer a powerful toolbox for tailoring the mechanical, electrical, and biological performance of next-generation bioinks aimed at functional tissue manufacturing.

2.3. Natural bioinks

Natural bioinks frequently used in bioprinting include collagen, alginate, gelatin, agarose, and hyaluronic acid [2, 23]. Natural bioinks are advantageous because they are biocompatible, closely mimic in vivo environments, and promote cellular activity such as adherence, maturation, differentiation, and proliferation [16, 28, 29]. From a biocompatibility and cell health perspective, natural bioinks seem to be the perfect group of materials for bioprinting, but natural hydrogels often lack the mechanical and rheological properties needed for constructs to keep their shape after bioprinting [2].

2.3.1. Matrigel

Matrigel is a natural material derived from the basement-membrane of Engelbreth-Holm-Swarm (EHS) mouse sarcoma, containing important components of the ECM surrounding tumors [3, 33]. Matrigel is frequently used in cancer cell culture because it closely mimics the in vivo environment consisting of laminin, collagen IV, and entactin among many other components [34-36]. Cancers most commonly start in epithelial cells, which grow on and interact with the basement-membrane. Cancer cells then have to penetrate the membrane to reach vasculature and spread throughout the body [37]. Due to the importance of the basement membrane in the development of cancer, Matrigel is a seemingly good material to choose, but the material composition varies from lot to lot, making it unreliable to use in experiments as it cannot be proven whether a change in cellular response is due to the variability in the material or the treatment given to the cells [35, 38]. Aside from Matrigel's variable composition, it can contain contaminants from mice, and it has poor mechanical and rheological properties meaning it cannot be printed on its own or produce large-scale products [33, 36].

2.3.2. Gelatin

Gelatin is a denatured protein, derived from collagen and is frequently used in bioprinting due to its non-toxic and non-immunogenic effect on cells, while also promoting cell adhesion and migration [13, 22, 39]. Like many other natural hydrogels, gelatin has poor mechanical properties; thus, it is frequently used in combination with other materials to increase its printability [22, 40]. Methacrylamide and methacrylate groups are frequently used with gelatin to improve its mechanical properties, while keeping its biocompatibility and biomimetic properties. When the methacrylamide and methacrylate groups are added the bioink becomes semi-synthetic and photocrosslinkable [41]. The improved mechanical properties, photocrosslinkability, and gelatin's ability to form gels at relatively low temperatures increase the shape fidelity of the printed construct [39]. Gelatin is also frequently used in combination with alginate, another natural hydrogel. Gelatin-alginate bioinks have the added benefit of increased biocompatibility and biomimetic properties, as well as allowing for multiple crosslinking agents to be used, slightly increasing the mechanical properties [42].

Table 2. Ideal bioink properties [2].

Property	Description
Printability	Properties that describe how the bioink is deposited and is impacted by multiple factors including rheological properties.
Biocompatibility	Cells and tissues should not be adversely affected by the material in use.
Degradation Kinetics	The rate at which the bioink degrades should be the same rate at which the cells are taking over the construct.
Structural and Mechanical	Materials used should be strong enough to support cellular activity and the weight of the bioprinted construct.
Biomimicry	The material properties should contribute to the microenvironment and be chosen with specific cell types or tissues in mind.

DOI: 10.62184/acj.jacj1000202524

2.3.3. Alginate

Alginate is another commonly used natural biomaterial that is derived from bacteria and marine algae [13, 22]. Alginate is biomimetic, promotes cell adhesion, and only creates a minimal inflammatory response [43]. While alginate's biological properties are not as favorable as those of gelatin or collagen, it has better mechanical properties, resulting in higher print fidelity [13, 22, 43]. Alginate can gel quickly when exposed to Ca^{2+}, often in the form of calcium chloride ($CaCl_2$), an ionic crosslinking agent [39, 42, 44]. Alginate is typically used in combination with other natural hydrogels to improve its biological properties [13]. To enhance the mechanical properties of hydrogels, alginate is often added to a blend to allow additional crosslinking methods to be utilized, such as UV crosslinking. Dual crosslinking creates more stable structures [43].

2.3.4. Collagen

Collagen is the most abundant protein in mammals, typically found in skin, bones, tendons, and connective tissue [25]. Collagen is a natural bioink and is classified into 28 different types, each type is given a Roman numeral [13]. Types I-III are the most prevalent in the human body [45]. Collagen type I is one of the most important components of the extracellular matrix and is used most often in bioprinting [22]. Collagen has many cell binding sites, high cell viability, and promotes cell proliferation [25], but hydrogels made with very high percentages of collagen lead to negative effects on cell proliferation and differentiation [45]. On its own, collagen has a low viscosity and weak mechanical properties, making it a poor candidate for bioprinting in its unmodified state [25, 45]. To allow for the printing of collagen, it is typically used in combination with other natural materials such as alginate, gelatin methacrylate, hyaluronic acid, or a combination of two or three materials [13, 25].

2.4. Synthetic bioinks

Synthetic bioinks come from man-made materials. The most commonly used synthetic bioinks include poly (ethylene glycol), poly (lactic acid), and poly (glycolic acid) [3]. While synthetic bioinks aren't as commonly used in bioprinting, they do have some advantages [22]. Synthetic bioinks have good mechanical properties for bioprinting and their mechanical and rheological properties can be tuned by changing the molecular weight. The disadvantages of synthetic bioinks are that they are generally not biomimetic, meaning they cannot support cellular activity on their own [2, 22, 33].

Poly(ethylene glycol) diacrylate (PEGDA) is a synthetic hydrogel synthesized by adding acrylate groups to both ends of the poly(ethylene glycol) (PEG) polymer and is available at a low cost [22, 46]. With properties such as high biocompatibility, low immunogenicity, and tunable mechanical properties, PEGDA is one of the most frequently used synthetic bioinks for bioprinting [22, 33, 46]. PEGDA is crosslinked using a photoinitiator along with exposure to UV light, a process that typically isn't toxic to cells [33, 47]. While PEGDA is biocompatible and non-toxic, it lacks biomimetic properties, meaning biological and chemical signaling molecules must be added in order to support cellular adhesion, proliferation and other activities [33]. Poly (L-lactic) acid is another synthetic material used as a bioink in bioprinting. Although it is not used as frequently as PEGDA, poly(L-lactic) acid is biocompatible and non- toxic. Like most other synthetic hydrogels, poly(L-lactic) acid is not biomimetic and cannot support cellular activity without the addition of biological factors [22]. A comparison of natural and synthetic bioinks can be seen in Table 3.

Table 3. Advantages and disadvantages of natural and synthetic bioinks [1, 2, 48, 49].

	Natural	Synthetic
Description	Derived from natural materials like plants and animals	Man-made
Advantages	• Biocompatible and usually biomimetic	• Tailorable to specific applications by changing functional groups and molecular weight • Non-immunogenic
Disadvantages	• Not tailorable	• Not biologically active

Advanced Carbon Journal, 2026, Vol. x, Iss. x, 165-190
DOI: 10.62184/acj.jacj1000202524

Review Article

3. Bioink characterization

Bioinks have been characterized in a variety of ways, including the investigation of rheological properties, mechanical properties, and degradation kinetics, as well as compression testing and swelling ratios. Of these, rheology is one of the most important in the ability to predict the quality of the resulting bioprinted construct [31].

3.1. Rheological properties

Rheology is the study of the deformation and flow of a material in response to applied forces [26]. These responses give insights on material behavior, including viscoelasticity and thixotropy [23]. The materials that are typically subject to rheological testing are those that are non-Newtonian, as Newtonian fluids have rheological properties that are independent of shear [23, 26]. The rheological properties of bioinks are studied because they are known to impact cell behavior such as proliferation and differentiation, and the overall performance and quality of the end 3D printed construct [23, 31, 50, 51]. Properties such as viscosity, viscoelastic shear moduli, viscosity recovery, and shear stress can be linked to a hydrogel's performance during all stages of printing [26, 52-54]. Bioinks must have a dominant elastic behavior, except during extrusion [23]. They must also be viscous enough to be extruded by a bioprinter and maintain their shape after being printed [31, 55]. Although its potential isn't always fully utilized in experimental work, rheology is an important tool used to evaluate properties that have impacts on the overall outcomes of printed constructs and the bioprinting process, which can be seen in Figure 5 [23, 26].

3.1.1. Viscoelastic properties

Bioinks are typically viscoelastic materials. The elastic or solid part of the material's behavior is described by the storage modulus (G'), also called the elastic modulus. The viscous or liquid part of the behavior is described by the loss or viscous modulus (G"). A balance between the storage and loss modulus is necessary for hydrogels to be able to produce quality 3D bioprinted constructs [26]. A dominant storage modulus is desirable for bioinks because the hydrogel must be able to maintain its shape after being printed [45]. Another measurement related to viscoelastic behavior is the loss factor (tan(δ)), which can be calculated by dividing the loss modulus by the storage modulus [26]. When the phase angle (δ) is equal to zero, the material is ideally elastic. Viscous materials have a phase angle of 90 degrees. Viscoelastic materials have a phase angle between 0 and 90 degrees [57]. Gao et al. found that bioinks with low loss factors have an increased print accuracy in the vertical (z) direction and a high loss factor resulted in increased print precision [26, 58].

3.1.2. Flow behavior

The flow behavior of bioinks is an important property to understand as it greatly affects how the material behaves during the bioprinting process. A material's flow behavior is a result of multiple material properties, including its viscoelastic properties and viscosity [23]. Bioinks with predominantly viscous behavior flow easily and are unable to maintain their shape. On the other hand, bioinks that are close to ideal elastic materials cannot be printed because they are brittle and will fracture under the stress of being extruded [23]. A happy medium is required for successful bioinks.

Viscosity, the resistance of fluid to flow under stress, is another important rheological property and is one of the most studied in relation to bioprinting [23, 26]. As a function of shear rate, viscosity can provide a lot of information on material behavior. Print accuracy, print fidelity, and extrudability are influenced by viscosity. High viscosity bioinks have been known to increase print accuracy and increase yield stress [26, 56]. When the viscosity of a material increases as the shear rate increases, the material is shear-thickening. When the viscosity decreases as the shear rate is increased, the material is shear-thinning. Shear-thinning occurs because the internal bonds of the material start to break as stress increases, causing the polymer chains to disentangle, allowing the material to flow more easily [23, 59]. High degrees of shear-thinning are associated with poor mechanical strength because the secondary bonds within the material structure are weak [60]. Shear-thinning and shear-thickening behaviors are time independent and are frequently modeled using the power law, Equation 1, also known as the Ostwald-de-Waele model, where $\eta(\dot{\gamma})$ is the viscosity, m is the consistency index, $\dot{\gamma}$ is the shear rate, and n is the flow index [26, 61].

$$\eta(\dot{\gamma}) = m\dot{\gamma}^{n-1} \qquad \textbf{(Equation 1 - Power Law)}$$

Advanced Carbon Journal, 2026, Vol. x, Iss. x, 165-190
DOI: 10.62184/acj.jacj1000202524

Review Article

Figure 5. Diagram of how rheological properties impact the bioprinting process [56]. Open access article distributed under the Creative Common Attribution License.

When the value of n is equal to one, then the material is Newtonian. The further the value is from one, the higher the degree of shear-thinning or shear-thickening. Values of n less than one indicate the material is shear-thinning and values of n greater than one indicate shear-thickening [23, 26]. Shear-thinning is an important property of bioinks. Shear-thinning bioinks prevent nozzle clogging in extrusion bioprinters, because the material flows more easily in the nozzle where stress is the highest and give the material the ability to be stacked on itself [62-64]. This property also reduces stress on cells during extrusion [23].

Viscosity recovery is another property related to flow behavior. Viscosity recovery is a measure of how viscosity changes with alternating periods of low and high shear stress [26]. During the first period, when the shear stress is low, it is expected that the bioink will have a relatively high viscosity. Then, during the period of high shear, the viscosity is expected to decrease due to its shear-thinning properties. The third period is one of low shear. If the viscosity during the third period reaches at least 80% of the original viscosity, then the material has sufficient viscosity recovery [23, 65]. Rapid and high viscosity recovery enables bioinks to flow through the nozzle easily and helps create constructs with higher print resolution and shape fidelity [52].

3.1.3. Yield stress

The yield stress, or yield point, of a hydrogel is the stress at which the hydrogel starts to flow [23, 26]. The Herschel-Bulkley law states that below the yield stress, the hydrogel will behave elastically, and above, the material behaves in accordance with the power law in Equation 1 [23]. In bioprinting, the yield stress of a bioink has multiple implications. The yield stress of a bioink is not only a predictor of the required printing pressure needed to extrude the bioink, but it can also be a telling sign of how well the bioink will be able to support the layers being stacked on itself [23, 30]. Bioinks with a very low yield stress are unable to support the weight of subsequently stacked layers which leads to low quality printed [23, 26, 52]. On the other hand, high yield stress enables the first printed layers to keep their shape and support each layer printed after [26]. The yield stress of a bioink is unaffected when cells are added [23].

3.2. Rheological testing

The testing used for rheological characterization in bioprinting consists of two types of measurements, continuous and oscillatory. Measurements are continuous if the shear rate as a function of time is constant [23]. During continuous measurements, stresses and shear rates are measured once steady state flow is reached after the respective stress or shear

rate is applied [23]. In oscillatory measurements shear stress or strain vary with time and either have a controlled stress or strain. Oscillatory measurements are used to look at time dependent behavior. Small-amplitude oscillatory shear (SAOS) measurements are used to investigate viscoelastic behavior, having the ability to look at the elastic behavior and viscous behavior separately [23].

3.2.1. Oscillation amplitude sweep

The oscillation amplitude sweep is an oscillatory test used to determine the linear viscoelastic region (LVR), which is the range of strain values where G' and G" act independently of strain [23, 26, 52]. The LVR is an important value to obtain at the beginning of rheological testing, as subsequent tests use strain as a constant parameter and it is important to ensure that G' and G" are independent of strain in other tests so the changes in viscoelastic behavior can be attributed to the independent variable instead of strain [23].

Oscillation amplitude sweeps are conducted by subjecting a hydrogel to a wide range of strains with a constant angular frequency [23]. Du et al. performed an oscillation amplitude sweep on their hydrogel with a gap of 200 μm at 25°C. They used a strain range of 0.01% to 100% and chose a fixed frequency of 1 rad/s [45]. Hu et al. selected a gap of 0.35 mm and a strain range of 0.01% to 500% with a fixed frequency of 10 rad/s [52]. The results of a standard oscillation amplitude sweep can be seen in Figure 6.

The linear viscoelastic range is the point at which the storage modulus starts to decrease, and the loss modulus starts to increase [52]. The point where G' and G" cross over is known as the flow point and is the point where the dominant behavior switches from being elastic to being viscous [23].

3.2.2. Oscillation frequency sweep

An oscillation frequency sweep is an oscillatory rheological test used to individually look at the storage and loss moduli as functions of frequency. This test allows for analysis of how G' and G" change with frequency and which behavior is dominant. In bioprinting, it is important that bioinks have a dominant elastic behavior, as a bioink's elasticity is one of the factors that allows it to maintain its shape after being bioprinted [23].

Oscillation frequency sweeps are conducted with a constant strain that is within the LVR, and a range of frequencies. Hu et al. performed their oscillation frequency sweep with a strain of 0.1% and a frequency range of 0.1 to 100 rad/s, the results of which can be seen in Figure 7 [52]. Minjares-Fuentes et al. performed the same test [61].

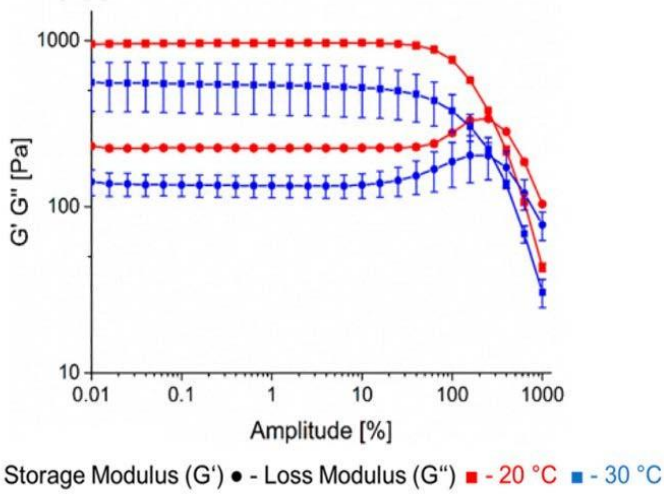

Figure 6. Results of an oscillation amplitude sweep performed on a bioink [66]. Open access article distributed under the Creative Commons Attribution License.

Advanced Carbon Journal, 2026, Vol. x, Iss. x, 165-190
DOI: 10.62184/acj.jacj1000202524

Review Article

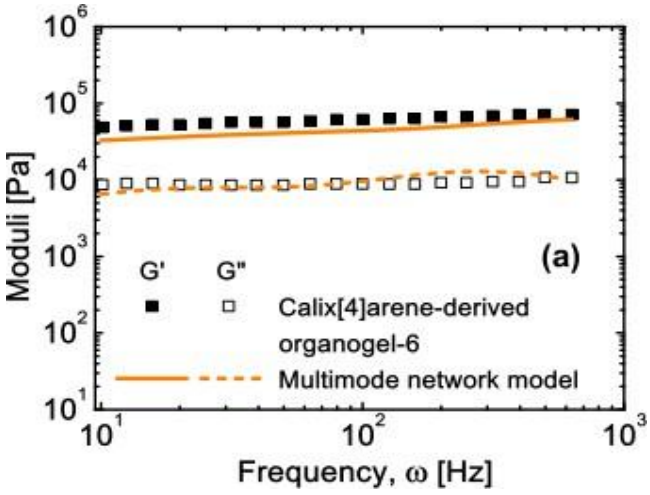

Figure 7. Results of an oscillation frequency sweep performed on a bioink. Adapted from Ref [67], copyright American Chemical Society.

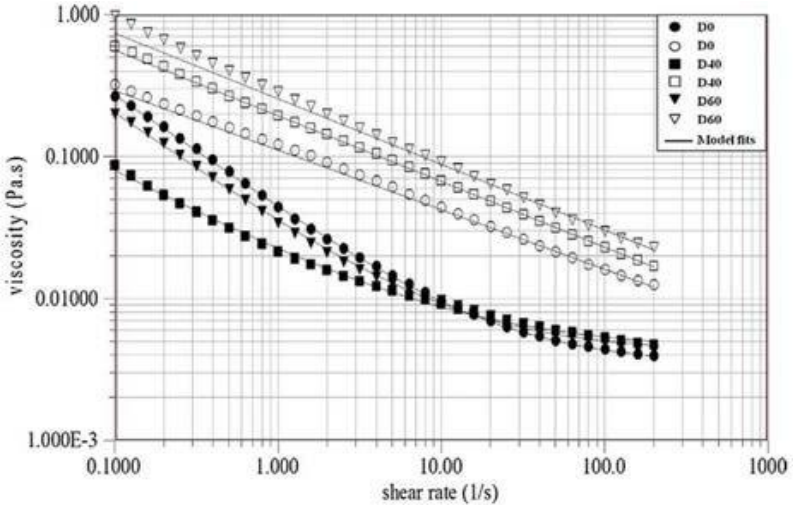

Figure 8. Results of a shear rate sweep preformed on a bioink. Adapted from Ref [61], copyright Elsevier.

When looking at the results of an oscillation frequency sweep, a storage modulus that is much greater than the loss modulus without the two crossing over indicates that bioink has a stable, solid-like behavior, which is ideal for bioinks because it allows the printed construct to keep its shape [23, 52]. This type of solid, frequency independent behavior is expected in gels due to their supramolecular structure [23].

3.2.3. Shear rate sweep

Shear rate sweeps are continuous measurements that examine how viscosity behaves as a function of shear rate [23]. This test is used to identify shear-thinning behavior. As discussed previously, a material has shear-thinning behavior if its viscosity decreases as shear rate is increased. This behavior can be seen in Figure 8.

Shear rate sweeps consist of subjecting the material to a range of shear rates while all other parameters are kept constant. Bociaga et al. chose a shear rate range from 0 to 160 1/s at room temperature [24]. Hu et al. and Minjares-Fuentes et al. used similar protocols but used shear rate ranges of 0.01 to 1000 1/s and 0.01 to 300 1/s, respectively [52, 61]. The decreasing line on a shear rate versus viscosity graph is indicative of shear-thinning behavior and is often modeled using the previously described power law.

3.2.4. Yield stress determination

A steady shear or strain sweep is used to study the yield point of a hydrogel [53]. During a steady shear rate sweep, the yield stress is defined as the stress at which viscosity decreases by several orders of magnitude. Yield stress can also be determined by performing a dynamic oscillatory stress sweep. In this test the yield stress is the point at which G' and G" crossover, indicating a change from dominantly elastic behavior to dominantly viscous behavior [52]. Minjares-Fuentes et al. conducted a steady shear sweep using a shear rate range of 0.1 to 300 1/s [61]. Ning et al. used a shear rate range of 0.1 to 1000 1/s to conduct a steady shear sweep [53].

3.2.5. Time sweep

Time sweeps are occasionally used to study if and how a hydrogels viscoelastic behavior changes over time as well as determining gelation time [23]. Flores-Torres et al. used a time sweep to determine gelation time. The hydrogel was loaded at 37°C and quickly cooled to 25°C to simulate the temperature change at the time of printing. The test was run for 2 hours, collecting G' and G" once every minute. The results showed that Matrigel accelerated the gelation process [68].

3.2.6. Viscosity recovery

The viscosity recovery test, also known as the three interval thixotropy test (3ITT), is used to measure how much of the material's original viscosity can be recovered after a period of high shear [23]. This is an important property to study in bioprinting as it allows the flow behavior of the bioink to be studied under conditions which mimic those of the bioprinting process [26].

The viscosity recovery test, which is a continuous measurement test, consists of alternating periods of low and high shear rate. The first period, one of low shear stress, is designed to mimic the conditions of the bioink in the printer cartridge prior to bioprinting. The next period is one of a high shear rate, which is meant to reflect the high shear rates that bioinks experience while being extruded through the printer nozzle. The last period, one of low stress is reflective of the bioink sitting statically on the print bed [23, 26, 69].

Hu et al. conducted a three interval thixotropy test, with periods of low shear were at a rate of 0.1 1/s and high shear rate at 100 1/s [52]. Davila et al. set the rest period shear rates to 1 1/s and high shear periods had various shear rates for different runs ranging from 50 1/s to 700 1/s [69]. As seen in Figure 9, when the shear rate increases, the viscosity decreases due to the shear- thinning properties of bioinks. It is the behavior of the viscosity after the shear rate has been greatly reduced that is important to the quantification of viscosity recovery. Ideal bioinks can fully recover their viscosity in a very short period of time, with adequate recovery being 80% [23, 65].

3.2.7. Temperature sweep

Temperature sweeps are oscillatory measurements used to investigate how a bioink's behavior changes when temperature is not constant. They can also be used to determine the sol- gel transition temperature, which helps find the temperature range at which the material behaves like a solid [23]. Du et al. cooled a bioink from 40°C to 4°C with a constant strain of 0.5% and an angular frequency of 1 rad/s [70]. Ning et al. also used cooling to study the effects of temperature change on a hydrogel, cooling it from 30°C to 5°C at a rate of -1°C/min with a constant frequency of 1 Hz and constant strain of 1% [53]. Park et al. also cooled hydrogels during the temperature sweep but did so at three different rates, 0.3°C/min, 0.6°C/min, 2.5°C/min, and 10°C/ min. This resulted in the conclusion that the higher the cooling rate, the lower the temperature needed to cause increases in G' and G" and to cause gelation. This result was also reflected with changes in heating rates [26, 71]. Hu et al. took the approach of heating the bioink and carried out the test under a constant frequency of 10 rad/s and a strain of 0.5%. The bioink was heated from 5°C to 45°C at a rate of 0.05°C/s [52]. It should be noted that the temperature should not be increased at a rate faster than 2°C/min, as the bioink may not fully reach the desired temperature [26, 72].

3.3. Print quality

As the field of bioprinting is relatively new, there has not been a consensus on how to quantify the overall quality of bioprinted constructs. The term 'printability' is frequently used when defining the quality of a bioprinted construct, but the definition varies greatly throughout the literature [23, 26, 73-78]. Some definitions of printability stem from rheological properties, while others are influenced by crosslinking, nozzle size, printed pore and bioink dimensions, how well the printed construct mimics the CAD model, filament spreading ratio, or the mechanical properties of the final printed construct [26, 73,

77, 79]. Bom et al. set forth some definitions for printability, extrudability, print accuracy, print fidelity, and print precision based on what was found in the literature, which can be seen in Table 4 [26]. These definitions and their applications in current literature will be discussed further in the later sections.

3.3.1. Printability

Printability is one of the most commonly used terms to describe bioprinted constructs in literature, but the term has a lot of ambiguity [26]. Bom et al. put forth the definition that printability is the ability of a bioink to be used to create a 3D construct layer by layer following a CAD model [26]. He et al. set forth two parameters for the definition of printability, including the ability to form filament and the ability be stacked in a layer by layer manner to create 3D structures as similar to the 3D model as possible [23, 73]. Li et al. do not give a quantitative definition of printability but state that it is determined by a combination of factors, including rheological properties, cross-linking, and printing parameters [74]. Naghieh et al. define printability as a hydrogel's ability to form a reproducible 3D printed construct that maintains its shape [75]. Gillispie et al. provide a rather abstract definition, defining printability as the ability to achieve desirable printing outcomes [80]. Godoi et al. state that the printability of a bioink depends on the bioink's material properties and crosslinking mechanisms [78].

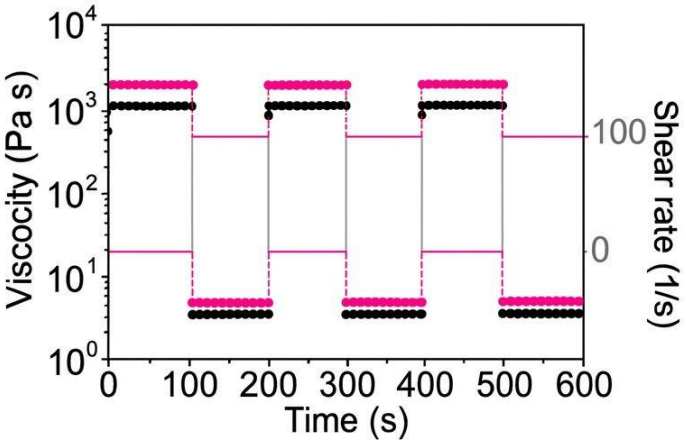

Figure 9. Results of a viscosity recovery test preformed on a bioink. Adapted from Ref [52], copyright IOP Publishing.

Table 4. Print quality terms and definitions. Adapted from Ref [26], copyright Elsevier.

Concept	Definition
Printability	The ability of a certain ink to achieve extrusion and maintain shape fidelity with high printing accuracy, which is influenced by pre-printing (rheological and nozzle features), printing (design, slicing, g-code (e.g., pressure, temperature and feed rate) and non-g-code parameters (e.g., environmental conditions)) and post- printing parameters (e.g., crosslinking, coating or drying techniques).
Extrudability	The capability of achieving extrusion, which is influenced by rheological parameters, printing parameters and environmental conditions.
Printing accuracy	Degree to which the 3D printed construct matches their size and spatial location, with respect to the original CAD model in terms of length, width, and height.
Printing fidelity	Degree to which the 3D printed construct matches their geometry with respect to the original design file in terms of length and width.
Printing precision	Measures the repeatability or reproducibility of a print in terms of size, geometry, and spatial location.

Advanced Carbon Journal, 2026, Vol. x, Iss. x, 165-190
DOI: 10.62184/acj.jacj1000202524

Review Article

Along with the multiple proposed definitions for printability, there are also multiple proposed tests to quantify printability. Ouyang et al. developed a test for quantifying printability. The test is conducted by printing a square grid and measuring the perimeter and area of each grid pore. The measurements are then used in the printability equation (Pr) where C is the circularity of an enclosed area ($C = 4\pi A\ L^2$), L is the perimeter, and A is for area shown in Equation 2. When using the printability equation, printability values closer to 1 indicate better printability as seen in Figure 10 [26, 36, 76, 77, 81, 82]. Naghieh uses multiple tests to measure printability. First, the strand diameter was calculated using the Equations 3, 4, and 5 where ρ is the density, Q is the flow rate, and D_S is the standard strand diameter [75].

Once the strand diameter was determined, strand printability was calculated using the strand printability equation in Equation 6 where Dexp is the experimental strand diameter. Values for strand printability closer to 1 indicate better strand printability [75].

3.3.2. Print accuracy

Print accuracy describes how well the printed construct matches the designed CAD model, including the size, shape, and location [26, 80]. Others have described print accuracy through a theoretical calculation called the Parameter Optimization Index (POI). The POI equation, Equation 7, considers factors such as nozzle gauge (D_G), printing pressure (p), and printed line thickness (t_{line}) [26, 31, 83]. Increased POI indicates greater print accuracy.

$$\mathrm{Pr} = \frac{\pi}{4} \times \frac{1}{\mathrm{C}} = \frac{L^2}{16A} \quad \textbf{(Equation 2 – Printability)}$$

$$\rho = \frac{Mass}{Volume} \quad \textbf{(Equation 3 – Density Equation)}$$

$$Q = \frac{Volume}{Time} \quad \textbf{(Equation 4 – Flow Rate Equation)}$$

$$\text{Nozzle speed} = \frac{4Q}{\pi\,(D_S)^2} \quad \textbf{(Equation 5 – Nozzle Speed Equation)}$$

$$\text{Strand printability} = \frac{D_S - D_{exp}}{D_S} \quad \textbf{(Equation 6 – Strand Printability Equation)}$$

$$POI = \frac{1}{t_{line} \times D_G \times \mathrm{p}} \quad \textbf{(Equation 7 – Parameter Optimization Index)}$$

Figure 10. Printability calculation. Adapted from Ref [76], copyright IOP Publishing.

Multiple tests have been used to quantify print accuracy. Kang et al. used unitless indexes of L', W', and H' to investigate the print accuracy of the length, width, and heigh of the construct, as seen in Figure 11. In the L' index equation, A is the average under printed length, B is the overlapping printed length, and C is the overprinted length. L' can range from zero to one, with a value of 1 indicating the best print accuracy. For equation W', W_{avg} is the average construct width and D is the nozzle diameter. In the H' index equation H is the construct height and T the average thickness [26, 84].

De Stefano et al., as well as Giuseppe, printed multiple single layer square grids with varying pore sizes. Photos were taken of the printed constructs and analyzed using ImageJ software. A print accuracy percentage calculation was then used to quantify the results. In the print accuracy equation, Equation 8, A_i is the printed area of each pore and A is the originally designed pore area, with high printer accuracy values indicating higher quality prints [31, 36].

DOI: 10.62184/acj.jacj1000202524

Review Article

$$\text{Printing Accuracy (\%)} = \left[1 - \frac{|A_i - A|}{A}\right] \times 100 \qquad \textbf{(Equation 8 – Print Accuracy Equation)}$$

$$W' = \frac{Wavg}{D}$$

$$L' = \frac{C}{A + B \cdot C}$$

$$H' = \frac{T}{H}$$

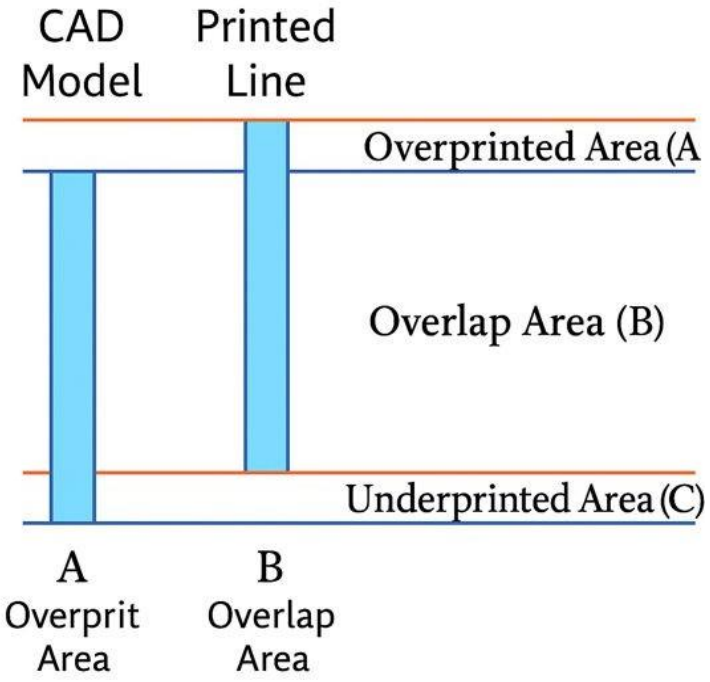

Figure 11. Kang's method for quantifying print accuracy [84].

3.3.3. Print fidelity

Print fidelity, also referred to as shape fidelity, is a printed construct's ability to retain its shape after being printed [26]. The rheological properties of yield stress and viscosity influence print fidelity. Higher yield stress and viscosity are associated with better shape fidelity because the bioink is more resistant to flow [23, 26, 85]. The main phenomenon that affects shape fidelity is bioink spreading, which is when the bioink spreads out and flattens once it is deposited on the print bed [26].

To investigate the shape fidelity of individually printed strands, Soltan et al. developed a strand uniformity test. The test consisted of printing multiple strands and imaging them. ImageJ was then used to measure the length of the outer edge. The uniformity factor equation in Figure 12 quantifies how similar the printed strand was to a perfect strand. Strands with a uniformity factor of 1 represent strands that are the same as the theoretical strand [26, 82].

He et al. used a grid to evaluate the print fidelity of grid structures (Figure 13). This test was conducted by printing a square pore with a known pore area (Art). Once the construct was bioprinted, the experimental pore area (Are) was calculated. The equation in Figure 13 is then used to calculate print fidelity [73].

Habib et al. used the same equation to calculate print fidelity to quantify printability [81].

3.3.4. Extrudability

Extrudability is another, less used, way to investigate whether a bioink can be bioprinted. Bom et al. defined extrudability as the ability of a bioink to be extruded from a bioprinter [26]. On the other hand, Gao et al. defined extrudability as the minimum pressure needed to extrude the bioink from the nozzle [58]. Others, while not directly referring to the property of extrudability, have tested extrudability in a qualitative way. O'Connell et al. state that if the bioink forms a droplet at the opening of the nozzle, then the bioink is not adequate to print.

This can be seen in Figure 14, side A is a bioink that cannot be adequately extruded, while the bioink on side B is extrudable [72]. Cooke et al. had similar observations when looking at the overall printability of their bioink [86].

Advanced Carbon Journal, 2026, Vol. x, Iss. x, 165-190
DOI: 10.62184/acj.jacj1000202524

Review Article

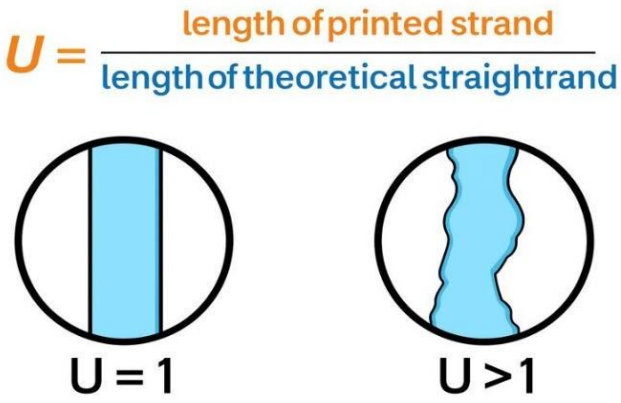

Figure 12. Uniformity factor equation with pictorial representation of a perfectly uniform strand and a non-uniform strand. Adapted from Ref [82], copyright American Chemical Society.

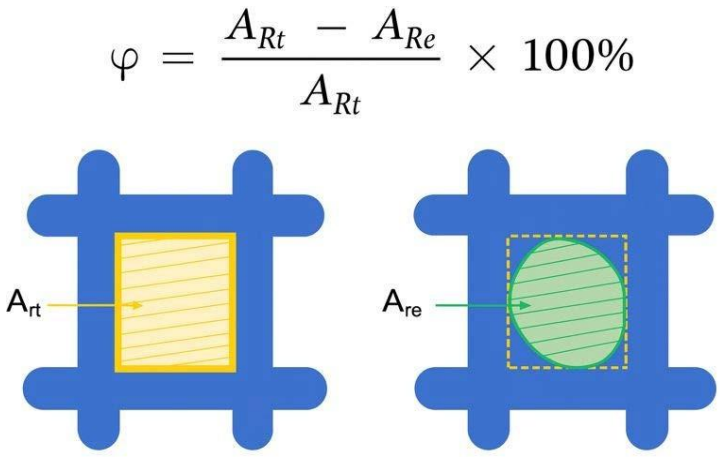

Figure 13. Print fidelity test for porous structures. Adapted from Ref [26], copyright Elsevier.

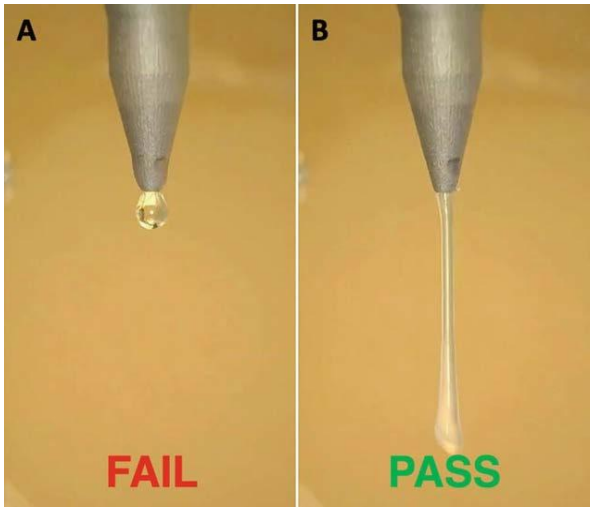

Figure 14. Qualitative extrudability test. Adapted from Ref [72], copyright Springer Science Business Media.

4. Applications of bioprinting

The ever-growing use of bioprinting in the tissue engineering field holds great promise of one day being able to print customized organs, tissues, and other biological constructs, as it combines the fields of medicine and engineering [87]. Bioprinting has been used in a variety of applications since its conception in 2002, including drug discovery and development, personalized tissue constructs, tissue vascularization, orthopedic research, cardiovascular research, dermatological applications, and cancer research.

4.1. Drug development and testing

Bioprinted constructs can be used for drug testing and development, which helps limit testing on animals and people. 3D cell cultures are used to mimic in vivo environments, which creates more accurate disease models [88, 89]. In 2017 a vascularized liver model was developed by Massa et al. to test possible drug toxicity. To achieve this, HepG2/C3A cells were printed to make a tissue model with channels that were seeded with human umbilical vein endothelial cells (HUVECs) [20]. Bhusal et al. used bioprinting to create microfluidic chips that mimic in vivo conditions. The microfluidic chips, shown in Figure 15, were used to deliver drugs to the embedded cells, and it was noted that there was a phenotypic change in the cell population [90].

Bioprinted constructs are also being used for drug testing on cardiovascular structures. Zhang et al. used a multistep process to create a heart on a chip in hopes of it being used for disease modeling or drug testing on cardiac tissue. Their process included printing endothelial cells, and then seeding the structure with cardiomyocytes. This enabled the formation of an endothelialized myocardium tissue. The tissue was then perfused using a microfluidic device [91].

4.1.1. Cancer drug development

During the development of new drugs, in vitro models are needed as predicate studies to animal testing and clinical trials. For cancer models specifically, 2D cultures are unable to mimic the hypoxic core that occurs due to the rapidly proliferating cancer cells. 3D models have been introduced as a way to overcome the discrepancies between 2D models and in vivo conditions, allowing in vitro studies to be more accurate and be more physiological relevant [16, 92]. Multiple types of 3D models have been introduced as better alternatives to the traditional 2D model in an attempt to get a more accurate drug response before moving to animal studies [16]. 3D models are superior in accurately representing the complexities of tumor microenvironment, including cellular behavior. The coculturing of multiple cell types in 3D models also adds to the biomimicry of tumor models as in vivo tumor microenvironments contain both cancerous and healthy, noncancerous cells [16, 36]. These 3D models have been found to be significantly better cancer models, especially for drug testing on personalized tumor models, which contain patient cells [16]. There are multiple types of 3D models. The most commonly used models include tumor spheroids, microfluidic devices, and bioprinted models [93].

Bioprinted models are a promising candidate for producing biomimetic 3D models for cancer drug testing, as there have been many advances in recent years [16, 93]. Unlike other 3D models, bioprinted models can be printed with precision, making them reproducible. Bioprinted models can take on more complex geometries and can be created with a larger range of sizes, while other models are limited to smaller sizes [3, 16, 36]. Other 3D models can adequately model the early stages of cancer, due to their simplicity and small size, but they fail to mimic the later stages of cancer. Bioprinted models overcome this limitation, allowing for the modeling of all stages of cancer to be bioprinted [3]. The formation of biomimetic 3D tumor models via bioprinting often requires two bioinks printed within one model, the cancer bioink and the stromal or noncancerous bioink. The cancer bioink in consists of a hydrogel, cancer cells, growth factors, and proteins [16, 94, 95]. The stromal bioink consists of the hydrogel of choice and healthy cell types that typically surround the cancer of study, which could include endothelial cells and fibroblasts [16, 96-98].

While 2D models are still most commonly used, many have worked toward improving bioprinted models. Swaminathan et al. compared constructs printed with bioinks containing spheroids and bioinks containing individual cells, finding that constructs printed with spheroids showed a greater resistance to the drug paclitaxel [16, 99]. Mollica et al. bioprinted tumor organoids to model breast cancer, noting that coculturing breast cancer cells with osteoblasts or mesenchymal stem cells increased the secretion of growth factor compared to traditional monoculture [16, 100, 101]. Dai et al. bioprinted a

construct with gelatin/alginate/fibrinogen bioink containing glioma stem cells to create a model for testing drug resistance. The results showed that glioma stem cells showed more drug resistance in 3D constructs than in traditional 2D models [102]. Flores-Torres et al. developed an alginate-gelatin-Matrigel bioink to print cancer spheroids, they then dissociated the printed spheroids in order to print multigenerational models, maintaining patient derived cancer spheroids. These bioprinted models were then used to test drug response [68]. Mao et al. created a grid-like construct with a gelatin-alginate-Matrigel hydrogel with intrahepatic cholangiocarcinoma cells. The tumor model showed the cells had a high survival rate and were actively proliferating as well as showing tumor markers consistent with a metastatic tumor [103]. Zhao et al. bioprinted Hela cells in a gelatin-alginate-fibrinogen hydrogel to create an in vitro cervical cancer model. The 3D model showed higher rates of proliferation, and the tendency to form spheroids, which does not occur in 2D models. The 3D models in this study also showed increased resistance to chemotherapy [102, 104].

4.2. Cardiovascular applications

Another common application of bioprinting is cardiovascular research. Cardiovascular disease is one of the leading causes of death across the world, [105] making medical advancements in the field a top priority. One current line of research is using 3D bioprinting to create heart valves that are superior to the current treatment options for patients with diseased valves [106]. Lueders et al. printed valve scaffolds and seeded the scaffolds with vascular cells to create functional valves that will one day be implantable, replacing diseased valves in human hearts [107]. Developing ways to incorporate vasculature into printed constructs, along with bioprinting blood vessels and vasculature for implantation, is another rapidly growing area of interest in the tissue engineering field. Much of the vasculature being printed in the past has lacked biocompatibility or the required structural integrity to be physiologically functional [108]. All tissues, bioprinted or natural, require vascularization to bring in oxygen and nutrients and remove waste [1]. If a tissue or organ lacks vasculature, the cells that make up the tissue become necrotic and die, limiting the growth and survival of the tissue [21, 109]. Bioprinting larger tissue constructs has been limited by internal vascularization, as cells must be within 100-200 μm of nutrient transfer [19, 110]. While a single vessel has been printed through a construct, this type of vasculature does not sufficiently provide nutrients or remove waste [20]. Lagatuz et al. used the open-source VESsel GENeration application to take 2D images of vascular tress to create and print 3D vessels that mimic in vivo vascular patterns [111]. Research is also being done in printing cardiovascular disease models to study the pathology and develop potential treatments. Harper et al. discussed using a patients' own cells and genome to bioprint personalized vascular constructs that are predicted to replace artificial and donor constructs in the future [112]. Jai et al. used a bioink consisting of gelatin Methacryloyl (GelMA), sodium alginate, and poly(-ethylene glycol)-tetra-acrylate (PEGTA). This bioink formulation was found to be biomimetic and had favorable characteristics for bioprinting. Jai then used a coaxial extrusion technique to print hollow tubes to mimic vasculature [17].

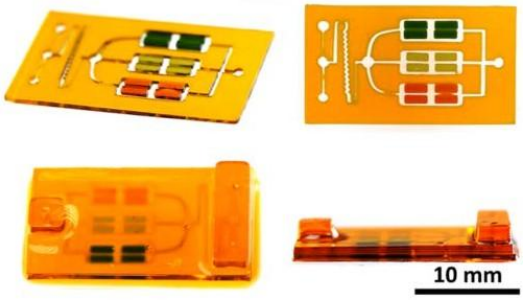

Figure 15. Bioprinted microfluidic chip is used for drug testing. Adapted from Ref [90], copyright ACS Publications.

4.3. Orthopedic applications

Orthopedic research has also found its place in the bioprinting field. Before the use of bioprinting, bone tissue engineering consisted of seeding cells on prefabricated scaffolds designed to support cell growth and waiting for the construct to become functional [113]. Zhai et al. used bioprinting technology to evenly distribute cells throughout the scaffold, while using a combination of 2 bioinks to achieve cell viability of more than 95%. The first ink consisted of polyethylene glycol diacrylate (PEGDA) and laponite XLG nano clay. The second ink consisted of hyaluronic acid sodium salt and rat osteoblasts. The two inks were printed in alternating layers to create the scaffold. The PEGDA and clay ink made the scaffold mechanically stable, while the hyaluronic acid and osteoblast ink was utilized to ensure even cell distribution throughout the scaffold and increased cell viability [6]. Similarly to Zhai, Murphy et al. used a dual ink printing process to create a scaffold with alternating layers of polycaprolactone (PLC) and bioactive borate glass composite with adipose stem cells in a Matrigel solution. Both the Matrigel and the PLC and borate bioinks provided conditions that not only supported cell growth, but were also angiogenic, poststimulatory, and anti-microbial. The combination of these properties shows great promise for future work in the bone tissue engineering field [5]. Lui et al. developed a bioink consisting of oligo(poly[ethylene glycol] fumarate) (OPF) and gelatin to create porous scaffolds for osteoblasts and neuronal cells. The gelatin was added in various concentrations to make a hydrogel that was able to be continuously extruded during printing. The gelatin was dissolved when the printed construct was placed in cell culture media, which created a porous scaffold that allowed for nutrients to reach the encapsulated cells more easily. Both the osteoblasts and neuronal cells showed high cell viability and good proliferation [87]. While there have been many advances in 3D bioprinting bone and cartilage tissue constructs, challenges are still being faced when trying to tailor the degradation rate of the bioink with cell growth. Another challenge is recapitulating the complexity of native tissue in a 3D bioprinted construct [113].

5. Summary and conclusions

In summary, there are multiple bioprinter types that are compatible with different carbon- based bioinks, the most common being the extrusion bioprinter. The hydrogels used for bioinks all have shortcomings. For some, it is poor material properties that limit the bioink's ability to be used when bioprinting large constructs because the bioink cannot support itself or the cellular activity that occurs within the construct. For others, it is limited or has no biocompatibility and biomimicry which inhibits cellular growth and proliferation, leading to cell death. In efforts to fix these shortcomings, two or more hydrogels are combined to form composite bioinks with good mechanical properties and good biological properties. Rheological testing has been used to determine if these bioinks are compatible with the bioprinting process, testing for material properties such as viscosity, yield stress, and viscoelasticity. These properties along with other printing parameters have been shown to affect the overall quality of the printed construct which is frequently called printability. There are many qualitative and quantitative definitions for printability as well as other commonly used terms like print accuracy and print fidelity. Some have introduced ways to quantify these values, but their methods are not widely used, making it difficult to compare printed constructs across multiple studies with different bioinks. Despite the lack of consensus on how best to describe the final printed construct, bioprinting has expanded into numerous areas of medicine, including drug development and testing, as well as cancer research.

Future research should focus on establishing standardized definitions and evaluation metrics for printed constructs to enable meaningful comparison across studies and to accelerate clinical translation.

Conflict of interest statement

The authors declare no conflict of interest.

Funding statement

This research received no external funding.

Author information

Corresponding Author: Anil Mahapatro*
E-mail: anil.mahapatro@wichita.edu
ORCID iD: 0009-0009-7111-9643
Author: Kami Bartholomew#
now known as Kami Olson

References

[1] Bishop, E. S., Mostafa, S., Pakvasa, M., Luu, H. H., …& Reid, R. R. (2017). 3-D bioprinting technologies in tissue engineering and regenerative medicine: Current and future trends. Genes & Diseases,4(4), 185-195. https://doi.org/10.1016/j.gendis.2017.10. 002

[2] Murphy, S. V., & Atala, A. (2014). 3D bioprinting of tissues and organs. Nature Biotechnology, 32(8), 773. https://doi.org/10.1038/nbt.2958

[3] Zhang, Y. S., Duchamp, M., Oklu, R., Ellisen, L.W., …& Khademhosseini, A. (2016). Bioprinting the cancer microenvironment. ACS Biomaterials Science & Engineering, 2(10), 1710-1721. https://doi.org/10.1021/acsbiomaterials.6b00246

[4] Aird, W. C. (2005). Spatial and temporal dynamics of the endothelium. Journal of Thrombosis and Haemostasis, 3(7), 1392-1406. https://doi.org/10.1111/j.15387836.2005.01328.x

[5] Murphy, C., Kolan, K., Li, W., Semon, J., …& Leu, M. (2017). 3D bioprinting of stem cells and polymer/bioactive glass composite scaffolds for bone tissue engineering. International Journal of Bioprinting, 3(1), 005. https://doi.org/10.18063/IJB.2017.01.005

[6] Zhai, X., Ruan, C., Ma, Y., Cheng, D., …& Lu, W. W. (2018). 3D-Bioprinted osteoblast-laden nanocomposite hydrogel constructs with induced microenvironments promote cell viability, differentiation, and osteogenesis both in vitro and in vivo. Advanced Science, 5(3), 1700550. https://doi.org/10.1002/advs.201700550

[7] Bhattacharyya, A., Priya, V. N. K., Kim, J.-h., Khatun, M. R., …& Noh, I. (2022). Nanodiamond enhanced mechanical and biological properties of extrudable gelatin hydrogel cross-linked with tannic acid and ferrous sulphate. Biomaterials Research, 26(1), 37. https://doi.org/doi:10.1186/s40824-022-00285-3

[8] Li, J., Liu, X., Crook, J. M., & Wallace, G. G. (2022). Development of 3D printable graphene oxide based bio-ink for cell support and tissue engineering. Frontiers in Bioengineering and Biotechnology, 10, 994776. https://doi.org/10.3389/fbioe.2022.994776

[9] Szymański, T., Semba, J. A., Mieloch, A. A., Cywoniuk, P., …& Rybka, J. D. (2023). Hyaluronic acid and multiwalled carbon nanotubes as bioink additives for cartilage tissue engineering. Scientific Reports, 13(1), 646. https://doi.org/10.1038/s41598-023-27901-z

[10] Kosowska, K., Korycka, P., Jankowska-Snopkiewicz, K., Gierałtowska, J., …& Klak, M. (2024). Graphene oxide (GO)-based bioink with enhanced 3D printability and mechanical properties for tissue engineering applications. Nanomaterials, 14(9), 760. https://doi.org/https:/doi.org/10.3390/nano14090760

[11] Liu, S., Ge, C., Li, Z., Shan, J., …& Zhang, X. (2024). Visible-light-induced silk fibroin hydrogels with carbon quantum dots as initiators for 3D bioprinting applications. ACS Biomaterials Science & Engineering, 10(9), 5822-5831. https://doi.org/10.1021/acsbiomaterials.4c01189

[12] Patil, R., & Alimperti, S. (2024). Graphene in 3D Bioprinting. Journal of Functional Biomaterials, 15(4), 82. https://doi.org/https:/doi.org/10.3390/jfb15040082

[13] Xu, J., Zheng, S., Hu, X., Li, L., …& Song, K. (2020). Advances in the research of bioinks based on natural collagen, polysaccharide and their derivatives for skin 3D bioprinting. Polymers, 12(6),1237. https://doi.org/10.3390/polym12061237

[14] Guillotin, B., & Guillemot, F. (2011). Cell patterning technologies for organotypic tissue fabrication. Trends in Biotechnology, 29(4), 183-190. https://doi.org/10.1016/j.tibtech.2010.12.008

[15] Jiang, T., Munguia-Lopez, J. G., Flores-Torres, S., Kort-Mascort, J., Kinsella, & J. M. (2019). Extrusion bioprinting of soft materials: An emerging technique for biological model fabrication. Applied Physics Reviews, 6. https://doi.org/10.1063/1.5059393

[16] Augustine, R., Kalva, S. N., Ahmad, R., Zahid, A. A., …& Hasan, A. (2021). 3D bioprinted cancer models: Revolutionizing personalized cancer therapy. Translational Oncology, 14(4), 101015. https://doi.org/10.1016/j.tranon.2021.101015

[17] Jia, W., Gungor-Ozkerim, P. S., Zhang, Y. S., Yue, K., …& Khademhosseini, A. (2016). Direct 3D bioprinting of perfusable vascular constructs using a blend bioink. Biomaterials, 106, 58-68. https://doi.org/10.1016/j.biomaterials.2016.07.038

[18] Kjar, A., McFarland, B., Mecham, K., Harward, N., & Huang, Y. (2021). Engineering of tissue constructs using

coaxial bioprinting. Bioactive Materials, 6(2), 460-471. https://doi.org/10.1016/j.bioactmat.2020.08.020

[19] Ze, Y., Li, Y., Huang, L., Shi, Y., …& Yao, Y. (2022). Biodegradable inks in indirect three- dimensional bioprinting for tissue vascularization. Frontiers in Bioengineering and Biotechnology, 10, 856398. https://doi.org/10.3389/fbioe.2022.856398

[20] Massa, S., Sakr, M. A., Seo, J., Bandaru, P., …& Shin, S. R. (2017). Bioprinted 3D vascularized tissue model for drug toxicity analysis. Biomicrofluidics, 11(4), 044109. https://doi.org/10.1063/1.4994708

[21] Kolesky, D. B., Truby, R. L., Gladman, A. S., Busbee, T. A., …& Lewis, J. A. (2014). 3D bioprinting of vascularized, heterogeneous cell-laden tissue constructs. Advanced Materials, 26(19), 3124-3130. https://doi.org/10.1002/adma.201305506

[22] Khoeini, R., Nosrati, H., Akbarzadeh, A., Eftekhari, A., …& Ozbolat, I. T. (2021). Natural and synthetic bioinks for 3D bioprinting. Advanced NanoBiomed Research, 1(8), 2000097. https://doi.org/10.1002/anbr.202000097

[23] Amorim, P. A., d'Ávila, M. A., Anand, R., Moldenaers, P., …& Bloemen, V. (2021). Insights on shear rheology of inks for extrusion-based 3D bioprinting. Bioprinting, 22, e00129. https://doi.org/10.1016/j.bprint.2021.e00129

[24] Bociaga, D., Bartniak, M., Grabarczyk, J., & Przybyszewska, K. (2019). Sodium alginate/gelatine hydrogels for direct bioprinting-the effect of composition selection and applied solvents on the bioink properties. Materials, 12(17), 2669. https://doi.org/10.3390/ma12172669

[25] Lan, X., Adesida, & A., Boluk, Y. (2022). Rheological and viscoelastic properties of collagens and their role in bioprinting by micro-extrusion. Biomedical Materials, 17(6), 062005. https://doi.org/10.1088/1748-605X/ac9b06

[26] Bom, S., Ribeiro, R., Ribeiro, H. M., Santos, C., & Marto, J. (2022). On the progress of hydrogel-based 3D printing: Correlating rheological properties with printing behaviour. International Journal of Pharmaceutics, 615, 121506. https://doi.org/10.1016/j.ijpharm.2022.121506

[27] Skardal, A., & Atala, A. (2015). Biomaterials for integration with 3-D bioprinting. Annals of Biomedical Engineering, 43(3), 730-746. https://doi.org/10.1007/s10439-014-1207-1

[28] Hospodiuk, M., Dey, M., Sosnoski, D., & Ozbolat, I. T. (2016). The bioink: A comprehensive review on bioprintable materials. Biotechnology Advances, 35(2), 217-239. https://doi.org/10.1016/j.biotechadv.2016.12.006

[29] Stanton, M. M., Samitier, J., & Sanchez, S. (2015). Bioprinting of 3D hydrogels. Lab on a Chip, 15(15), 3111-3115. https://doi.org/10.1039/c5lc90069g

[30] Rosenzweig, M. E. C. D. H. (2021). The rheology of direct and suspended extrusion bioprinting. Biophysics of Biofabrication, 5(1). https://doi.org/https:/doi.org/10.1063/5.0031475

[31] Giuseppe, M. D., Law, N., Webb, B., Macrae, R. A., …& Doyle, B. J. (2018). Mechanical behaviour of alginate-gelatin hydrogels for 3D bioprinting. Journal of The Mechanical Behavior of Biomedical Materials, 79, 150-157. https://doi.org/10.1016/j.jmbbm.2017.12.018

[32] Bartholomew, K., & Mahapatro, A. (2025). Rheological characterization and print quality studies of gelatin/collagen I/PEGDA hydrogels. International Journal of Polymeric Materials and Polymeric Biomaterials, 74(11), 975-986. https://doi.org/10.1080/00914037.2024.2391964

[33] Aisenbrey, E. A., & Murphy, W. L. (2020). Synthetic alternatives to Matrigel. Nature Reviews Materials, 5(7), 539-551. https://doi.org/10.1038/s41578-020-0199-8

[34] Borries, M., Barooji, Y. F., Yennek, S., Grapin-Botton, A., …& Oddershede, L. B. (2020). Quantification of visco-elastic properties of a matrigel for organoid development as a function of polymer concentration. Frontiers in Physics, 8, 579168. https://doi.org/10.3389/fphy.2020.579168

[35] Hughes, C. S., Postovit, L. M., & Lajoie, G. A. (2010). Matrigel: A complex protein mixture required for optimal growth of cell culture. Proteomics, 10(9), 1886-1890. https://doi.org/10.1002/pmic.200900758

[36] De Stefano, P., Briatico-Vangosa, F., Bianchi, E., Pellegata, A. F., …& Dubini, G. (2021). Bioprinting of matrigel scaffolds for cancer research. Polymers, 13(12), 2026. https://doi.org/10.3390/polym13122026

[37] Chang, J., & Chaudhuri, O. (2019). Beyond proteases: Basement membrane mechanics and cancer invasion. Journal of Cell Biology, 218(8), 2456-2469. https://doi.org/10.1083/jcb.201903066

[38] Van Zundert, I., Fortuni, B., & Rocha, S. (2020). From 2D to 3D cancer cell models- The enigmas of drug delivery

research. Nanomaterials, 10(11), 2236. https://doi.org/10.3390/nano10112236

[39] Wang, X., Ao, Q., Tian, X., Fan, J., …& Bai, S. (2017). Gelatin-Based Hydrogels for Organ 3D Bioprinting. Polymers, 9(9), 401. https://doi.org/10.3390/polym9090401

[40] Labowska, M. B., Cierluk, K., Jankowska, A. M., Kulbacka, J., …& Michalak, I. (2021). A review on the adaption of alginate-gelatin hydrogels for 3D cultures and bioprinting. Materials, 14(4), 858. https://doi.org/10.3390/ma14040858

[41] Pepelanova, I., Kruppa, K., Scheper, T., & Lavrentieva, A. (2018). Gelatin-methacryloyl (GelMA) hydrogels with defined degree of functionalization as a versatile toolkit for 3D cell culture and extrusion bioprinting. Bioengineering, 5(3), 55. https://doi.org/10.3390/bioengineering5030055

[42] Chen, Q., Tian, X., Fan, J., Tong, H., …& Wang, X. (2020). An interpenetrating alginate/gelatin network for three-dimensional (3D) cell cultures and organ bioprinting. Molecules, 25(3), 756. https://doi.org/10.3390/molecules25030756

[43] Gopinathan, J., & Noh, I. (2018). Recent trends in bioinks for 3D printing. Biomaterials Research, 22(1), 11. https://doi.org/10.1186/s40824-018-0122-1

[44] Blanco-Fernandez, B., Rey-Vinolas, S., Bagci, G., Rubi-Sans, G., …& Engel, E. (2022). Bioprinting decellularized breast tissue for the development of three-dimensional breast cancer models. ACS Applied Materials & Interfaces, 14(26), 29467-29482. https://doi.org/10.1021/acsami.2c00920

[45] Stepanovska, J., Supova, M., Hanzalek, K., Broz, A., & Matejka, R. (2021). Collagen bioinks for bioprinting: A systematic review of hydrogel properties, bioprinting parameters, protocols, and bioprinted structure characteristics. Biomedicines, 9(9), 1137. https://doi.org/10.3390/biomedicines9091137

[46] Malo de Molina, P., Lad, S., & Helgeson, M. E. (2015). Heterogeneity and its influence on the properties of difunctional poly(ethylene glycol) hydrogels: Structure and mechanics. Macromolecules, 48(15), 5402- 5411. https://doi.org/10.1021/acs.macromol.5b01115

[47] Hamedi, E., Vahedi, N., Sigaroodi, F., Parandakh, A., …& Khani, M. M. (2023). Recent progress of bio-printed PEGDA-based bioinks for tissue regeneration. Polymers for Advanced Technologies, 34(11), 3505-3517. https://doi.org/10.1002/pat.6164

[48] Irvine, S. A., & Venkatraman, S. S. (2016). Bioprinting and differentiation of stem cells. Molecules, 21(9), 1188. https://doi.org/10.3390/molecules21091188

[49] Gao, G., Cui, X. (2016). Three-dimensional bioprinting in tissue engineering and regenerative medicine. Biotechnology Letters, 38(2), 203-211. https://doi.org/10.1007/s10529-015-1975-1

[50] Chaudhuri, O., Gu, L., Klumpers, D., Darnell, M., …& Mooney, D. J. (2016). Hydrogels with tunable stress relaxation regulate stem cell fate and activity. Nature Materials, 15(3), 326-334. https://doi.org/10.1038/nmat4489

[51] Nam, S., Stowers, R., Lou, J., Xia, Y., & Chaudhuri, O. (2019). Varying PEG density to control stress relaxation in alginate-PEG hydrogels for 3D cell culture studies. Biomaterials, 200, 15-24. https://doi.org/10.1016/j.biomaterials.2019.02.004

[52] Hu, C., Ahmad, T., Haider, M. S., Hahn, L., …& Luxenhofer, R. (2022). A thermogelling organic-inorganic hybrid hydrogel with excellent printability, shape fidelity and cytocompatibility for 3D bioprinting. Biofabrication, 14(2), 025005. https://doi.org/10.1088/1758-5090/ac40ee

[53] Ning, L., Mehta, R., Cao, C., Theus, A., …& Serpooshan, V. (2020). Embedded 3D bioprinting of gelatin methacryloyl-based constructs with highly tunable structural fidelity. ACS Applied Materials & Interfaces, 12(40), 44563-44577. https://doi.org/10.1021/acsami.0c15078

[54] Spencer, A. R., Shirzaei Sani, E., Soucy, J. R., Corbet, C. C., …& Annabi, N. (2019). Bioprinting of a cell-laden conductive hydrogel composite. ACS Applied Materials & Interfaces, 11(34), 30518- 30533. https://doi.org/10.1021/acsami.9b07353

[55] Chung, J. H. Y., Naficy, S., Yue, Z., Kapsa, R., …& Wallace, G. G. (2013). Bio-ink properties and printability for extrusion printing living cells. Biomaterials Science, 1(7), 763-773. https://doi.org/10.1039/c3bm00012e

[56] Schwab, A., Levato, R., D'Este, M., Piluso, S., …& Malda, J. (2020). Printability and shape fidelity of bioinks in 3D bioprinting. Chemical Reviews, 120(19), 11028-11055. https://doi.org/10.1021/acs.chemrev.0c00084

[57] Ghanbari, A., Mousavi, Z., Heuzey, M. C., Patience, G. S., & Carreau, P. J. (2020). Experimental methods in chemical

engineering: Rheometry. The Canadian Journal of Chemical Engineering, 98(7), 1456-1470. https://doi.org/10.1002/cjce.23749

[58] Gao, T., Gillispie, G. J., Copus, J. S., Pr, A. K., …& Lee, S. J. (2018). Optimization of gelatin-alginate composite bioink printability using rheological parameters: A systematic approach. Biofabrication, 10(3), 034106. https://doi.org/10.1088/1758-5090/aacdc7

[59] Patel, P. N., Smith, C. K., & Patrick Jr, C. W. (2005). Rheological and recovery properties of poly(ethylene glycol) diacrylate hydrogels and human adipose tissue. Journal of Biomedical Materials Research Part A, 73(3), 313-319. https://doi.org/10.1002/jbm.a.30291

[60] Unal, A. Z., & West, J. L. (2020). Synthetic ECM: Bioactive synthetic hydrogels for 3D tissue engineering. Bioconjugate Chemistry, 31(10), 2253-2271. https://doi.org/10.1021/acs.bioconjchem.0c00270

[61] Minjares-Fuentes, R., Medina-Torres, L., González-Laredo, R. F., Rodríguez-González, V. M., …& Femenia, A. (2017). Influence of water deficit on the main polysaccharides and the rheological properties of Aloe vera (*Aloe barbadensis Miller*) mucilage. Industrial Crops and Products, 109, 644-653. https://doi.org/10.1016/j.indcrop.2017.09.016

[62] Asohan, A. W., Hashim, R., Ku Ishak, K. M., Abdul Hamid, Z. A., …& Bustami, Y. (2022). Preparation and characterisation of cellulose nanocrystal/alginate/polyethylene glycol diacrylate (CNC/Alg/PEGDA) hydrogel using double network crosslinking technique for bioprinting application. Applied Sciences, 12(2), 771. https://doi.org/10.3390/app12020771

[63] Wang, X., Ao, Q., Tian, X., Fan, J., …& Bai, S. (2016). 3D bioprinting technologies for hard tissue and organ engineering. Materials, 9(10), 802. https://doi.org/10.3390/ma9100802

[64] Van Den Bulcke, A. I., Bogdanov, B., De Rooze, N., Schacht, E. H., …& Berghmans, H. (2000). Structural and rheological properties of methacrylamide modified gelatin hydrogels. Biomacromolecules, 1(1), 31-38. https://doi.org/10.1021/bm990017d

[65] Peak, C. W., Stein, J., Gold, K. A., & Gaharwar, A. K. (2018). Nanoengineered colloidal inks for 3D bioprinting. Langmuir, 34(3), 917-925. https://doi.org/10.1021/acs.langmuir.7b02540

[66] Bottcher, B., Pflieger, A., Schumacher, J., Jungnickel, B., & Feller, K. H. (2022). 3D bioprinting of prevascularized full-thickness gelatin-alginate structures with embedded co-cultures. Bioengineering, 9(6), 242. https://doi.org/10.3390/bioengineering9060242

[67] Ramya, K. A., Reddy, S. M. M., Shanmugam, G., & Deshpande, A. P. (2020). Fibrillar network dynamics during oscillatory rheology of supramolecular gels. Langmuir, 36(44), 13342-13355. https://doi.org/10.3390/bioengineering9060242

[68] Flores-Torres, S., Peza-Chavez, O., Kuasne, H., Munguia-Lopez, J. G., …& Kinsella, J. M. (2021). Alginate-gelatin-Matrigel hydrogels enable the development and multigenerational passaging of patient-derived 3D bioprinted cancer spheroid models. Biofabrication, 13(2), 025001. https://doi.org/10.1088/1758-5090/abdb87

[69] Dávila, J. L., & d'Ávila, M. A. (2018). Rheological evaluation of Laponite/alginate inks for 3D extrusion- based printing. The International Journal of Advanced Manufacturing Technology, 101(1), 675-686. https://doi.org/10.1007/s00170-018-2876-y

[70] Du, H., Wang, L., Lu, K., Pan, B., & Liu, J. (2022). YAFAF-based hydrogel: Characterization, mechanism, and factors influencing micro-organization. Journal of Agricultural and Food Chemistry, 70(34), 10669-10679. https://doi.org/10.1021/acs.jafc.2c04505

[71] Park, J., Lee, S. J., Chung, S., Lee, J. H., …& Park, S. A. (2017). Cell-laden 3D bioprinting hydrogel matrix depending on different compositions for soft tissue engineering: Characterization and evaluation. Materials Science and Engineering: C, 71, 678-684. https://doi.org/10.1016/j.msec.2016.10.069

[72] O'Connell, C., Ren, J., Pope, L., Zhang, Y., …& Onofrillo, C. (2020). Correction to: Characterizing bioinks for extrusion bioprinting: Printability and rheology. Methods in Molecular Biology, 2140, C1. https://doi.org/10.1007/978-1-0716-0520-2_18

[73] He, Y., Yang, F., Zhao, H., Gao, Q., …& Fu, J. (2016). Research on the printability of hydrogels in 3D bioprinting. Scientific Reports, 6(1), 29977. https://doi.org/10.1038/srep29977

[74] Li, J., Wu, C., Chu, P. K., & Gelinsky, M. (2020). 3D printing of hydrogels: Rational design strategies and emerging

biomedical applications. Materials Science and Engineering: R: Reports, 140, 100543. https://doi.org/10.1016/j.mser.2020.100543

[75] Naghieh, S., Sarker, M. D., Sharma, N. K., Barhoumi, Z., & Chen, X. (2019). Printability of 3D printed hydrogel scaffolds: Influence of hydrogel composition and printing parameters. Applied Sciences, 10(1), 292. https://doi.org/10.3390/app10010292

[76] Ouyang, L., Yao, R., Zhao, Y., & Sun, W. (2016). Effect of bioink properties on printability and cell viability for 3D bioplotting of embryonic stem cells. Biofabrication, 8(3), 035020. https://doi.org/10.1088/1758-5090/8/3/035020

[77] Cai, F. F., Heid, S., & Boccaccini, A. R. (2021). Potential of Laponite® incorporated oxidized alginate- gelatin (ADA-GEL) composite hydrogels for extrusion-based 3D printing. Journal of Biomedical Materials Research Part B: Applied Biomaterials, 109(8), 1090-1104. https://doi.org/10.1002/jbm.b.34771

[78] Godoi, F. C., Prakash, S., & Bhandari, B. R. (2016). 3D printing technologies applied for food design: Status and prospects. Journal of Food Engineering, 179, 44-54. https://doi.org/10.1016/j.jfoodeng.2016.01.025

[79] Freeman, F. E., & Kelly, D. J. (2017). Tuning alginate bioink stiffness and composition for controlled growth factor delivery and to spatially direct MSC fate within bioprinted tissues. Scientific Reports, 7(1), 17042. https://doi.org/10.1038/s41598-017-17286-1

[80] Gillispie, G., Prim, P., Copus, J., Fisher, J., …& Lee, S. J. (2020). Assessment methodologies for extrusion-based bioink printability. Biofabrication, 12(2), 022003. https://doi.org/10.1088/1758-5090/ab6f0d

[81] Habib, A., Sathish, V., Mallik, S., & Khoda, B. (2018). 3D printability of alginate-carboxymethyl cellulose hydrogel. Materials, 11(3), 454. https://doi.org/10.3390/ma11030454

[82] Soltan, N., Ning, L., Mohabatpour, F., Papagerakis, P., & Chen, X. (2019). Printability and cell viability in bioprinting alginate dialdehyde-gelatin scaffolds. ACS Biomaterials Science & Engineering, 5(6), 2976-2987. https://doi.org/10.1021/acsbiomaterials.9b00167

[83] Webb, B., & Doyle, B. J. (2017). Parameter optimization for 3D bioprinting of hydrogels. Bioprinting, 8, 8-12. https://doi.org/10.1016/j.bprint.2017.09.001

[84] Kang, K. H., Hockaday, L. A., & Butcher, J. T. (2013). Quantitative optimization of solid freeform deposition of aqueous hydrogels. Biofabrication, 5(3), 035001. https://doi.org/10.1088/1758-5082/5/3/035001

[85] Mouser, V. H., Melchels, F. P., Visser, J., Dhert, W. J., …& Malda, J. (2016). Yield stress determines bioprintability of hydrogels based on gelatin-methacryloyl and gellan gum for cartilage bioprinting. Biofabrication, 8(3), 035003. https://doi.org/10.1088/1758-5090/8/3/035003

[86] Cooke, M. E., & Rosenzweig, D. H. (2021). The rheology of direct and suspended extrusion bioprinting. APL Bioengineering, 5(1), 011502. https://doi.org/10.1063/5.0031475

[87] Liu, X., Gaihre, B., George, M. N., Miller, A. L., …& Lu, L. (2021). 3D bioprinting of oligo(poly[ethylene glycol] fumarate) for bone and nerve tissue engineering. Journal of Biomedical Materials Research Part A, 109(1), 6-17. https://doi.org/10.1002/jbm.a.37002

[88] Fang, Y., & Eglen, R. M. (2017). Three-dimensional cell cultures in drug discovery and development. Slas Discovery: Advancing Life Sciences R&D, 22(5), 456-472. https://doi.org/10.1177/1087057117696795

[89] Nothdurfter, D., Ploner, C., Coraca-Huber, D. C., Wilflingseder, D., …& Ausserlechner, M. J. (2022). 3D bioprinted, vascularized neuroblastoma tumor environment in fluidic chip devices for precision medicine drug testing. Biofabrication, 14(3), 035002. https://doi.org/10.1088/1758-5090/ac5fb7

[90] Bhusal, A., Dogan, E., Nieto, D., Mousavi Shaegh, S. A., …& Miri, A. K. (2022). 3D bioprinted hydrogel microfluidic devices for parallel drug screening. ACS Applied Bio Materials, 5(9), 4480-4492. https://doi.org/10.1021/acsabm.2c00578

[91] Zhang, Y. S., Arneri, A., Bersini, S., Shin, S. R., …& Khademhosseini, A. (2016). Bioprinting 3D microfibrous scaffolds for engineering endothelialized myocardium and heart-on-a-chip. Biomaterials, 110, 45-59. https://doi.org/10.1016/j.biomaterials.2016.09.003

[92] Al Tameemi, W., Dale, T. P., Al-Jumaily, R. M. K., & Forsyth, N. R. (2019). Hypoxia-modified cancer cell metabolism. Frontiers in Cell and Developmental Biology, 7, 4. https://doi.org/10.3389/fcell.2019.00004

[93] Datta, P., Dey, M., Ataie, Z., Unutmaz, D., & Ozbolat, I. T. (2020). 3D bioprinting for reconstituting the cancer microenvironment. NPJ Precision Oncology, 4(1), 18, https://doi.org/10.1038/s41698-020-0121-2

[94] Micalizzi, D. S., Maheswaran, S., & Haber, D. A. (2017). A conduit to metastasis: Circulating tumor cell biology. Genes & Development, 31(18), 1827-1840. https://doi.org/10.1101/gad.305805.117

[95] Lei, M., & Wang, X. (2016). Biodegradable polymers and stem cells for bioprinting. Molecules, 21(5), 539. https://doi.org/10.3390/molecules21050539

[96] Yin, Z., Dong, C., Jiang, K., Xu, Z., …& Wang, L. (2019). Heterogeneity of cancer- associated fibroblasts and roles in the progression, prognosis, and therapy of hepatocellular carcinoma. Journal of Hematology & Oncology, 12(1), 101. https://doi.org/10.1186/s13045-019-0782-x

[97] Prager, B. C., Xie, Q., Bao, S., & Rich, J. N. (2019). Cancer stem cells: The architects of the tumor ecosystem. Cell Stem Cell, 24(1), 41-53. https://doi.org/10.1016/j.stem.2018.12.009

[98] Gungor-Ozkerim, P. S., Inci, I., Zhang, Y. S., Khademhosseini, A., & Dokmeci, M. R. (2018). Bioinks for 3D bioprinting: An overview. Biomaterials Science, 6(5), 915-946. https://doi.org/10.1039/c7bm00765e

[99] Swaminathan, S., Hamid, Q., Sun, W., & Clyne, A. M. (2019). Bioprinting of 3D breast epithelial spheroids for human cancer models. Biofabrication, 11(2), 025003. https://doi.org/10.1088/1758-5090/aafc49

[100] Mollica, P. A., Booth-Creech, E. N., Reid, J. A., Zamponi, M., …& Bruno, R. D. (2019). 3D bioprinted mammary organoids and tumoroids in human mammary derived ECM hydrogels. Acta Biomaterialia, 95, 201-213. https://doi.org/10.1016/j.actbio.2019.06.017

[101] Zhou, X., Zhu, W., Nowicki, M., Miao, S., …& Zhang, L. G. (2016). 3D bioprinting a cell-laden bone matrix for breast cancer metastasis study. ACS Applied Materials & Interfaces, 8(44), 30017-30026. https://doi.org/10.1021/acsami.6b10673

[102] Dai, X., Ma, C., Lan, Q., & Xu, T. (2016). 3D bioprinted glioma stem cells for brain tumor model and applications of drug susceptibility. Biofabrication, 8(4), 045005. https://doi.org/10.1088/1758-5090/8/4/045005

[103] Mao, S., He, J., Zhao, Y., Liu, T., …& Sun, W. (2020). Bioprinting of patient- derived in vitro intrahepatic cholangiocarcinoma tumor model: Establishment, evaluation and anti-cancer drug testing. Biofabrication, 12(4), 045014. https://doi.org/10.1088/1758-5090/aba0c3

[104] Zhao, Y., Yao, R., Ouyang, L., Ding, H., …& Sun, W. (2014). Three- dimensional printing of Hela cells for cervical tumor model in vitro. Biofabrication, 6(3), 035001. https://doi.org/10.1088/1758-5082/6/3/035001

[105] Khanna, A., Ayan, B., Undieh, A. A., Yang, Y. P., & Huang, N. F. (2022). Advances in three-dimensional bioprinted stem cell-based tissue engineering for cardiovascular regeneration. Journal of Molecular and Cellular Cardiology, 169, 13- 27. https://doi.org/10.1016/j.yjmcc.2022.04.017

[106] Jana, S., Tefft, B. J., Spoon, D. B., & Simari, R. D. (2014). Scaffolds for tissue engineering of cardiac valves. Acta Biomaterialia, 10(7), 2877-2893. https://doi.org/10.1016/j.actbio.2014.03.014

[107] Lueders, C., Jastram, B., Hetzer, R., & Schwandt, H. (2014). Rapid manufacturing techniques for the tissue engineering of human heart valves. European Journal of Cardio-Thoracic Surgery, 46(4), 593-601. https://doi.org/10.1093/ejcts/ezt510

[108] Schoneberg, J., De Lorenzi, F., Theek, B., Blaeser, A., …& Fischer, H. (2018). Engineering biofunctional in vitro vessel models using a multilayer bioprinting technique. Scientific Reports, 8(1), 10430. https://doi.org/10.1038/s41598-018-28715-0

[109] Liu, Y., Zhang, Y., Mei, T., Cao, H., …& Liu, Z. (2022). hESCs-derived early vascular cell spheroids for cardiac tissue vascular engineering and myocardial infarction treatment. Advanced Science, 9(9), 2104299. https://doi.org/10.1002/advs.202104299

[110] Malheiro, A., Wieringa, P., Mota, C., Baker, M., & Moroni, L. (2016). Patterning vasculature: The role of biofabrication to achieve an integrated multicellular ecosystem. ACS Biomaterials Science & Engineering, 2(10), 1694-1709. https://doi.org/10.1021/acsbiomaterials.6b00269

[111] Lagatuz, M., Vyas, R. J., Predovic, M., Lim, S., …& Parsons-Wingerter, P. (2021). Vascular patterning as integrative readout of complex molecular and physiological

signaling by vessel generation analysis. Journal of Vascular Research, 58(4), 207-230. https://doi.org/10.1159/000514211

[112] Harper, R. L., Ferrante, E. A., & Boehm, M. (2022). Development of vascular disease models to explore disease causation and pathomechanisms of rare vascular diseases. Seminars in Immunopathology, 44(3), 259-268. https://doi.org/10.1007/s00281-022-00925-9

[113] Yang, J., Zhang, Y. S., Yue, K., & Khademhosseini, A. (2017). Cell-laden hydrogels for osteochondral and cartilage tissue engineering. Acta Biomaterialia, 57, 1-25. https://doi.org/10.1016/j.actbio.2017.01.036